Active Fault-Tolerant Control for Path Following of Unmanned Surface Vehicle

Yinsong Qu
College of Intelligent Systems Science and Engineering
Harbin Engineering University
Harbin, China
qu13298110549@163.com

Tian Xia
Warship Manufacturing Technology R&D Department
Shanghai Shipbuilding Technology Research Institute
Shanghai, China
921803279@qq.com

Abstract—**In this paper a solution to the problem of active fault-tolerant control for path following of underactuated surface vessels with rudderless double thrusters is studied. The control method proposed can guarantee that the underactuated surface vessels accurately follow the given path even in case of partial gain loss of the actuator. The closed-loop system is verified to be uniformly bounded by Lyapunov stability theory. Finally, the simulation experiment is presented to display that the developed fault-tolerant control method is effective in fault detection, estimation, and controller reconfiguration for cancelling the adverse effects of gain loss of thrusters in path following task.**

Keywords—path following, active fault-tolerant control, Backstepping method, unmanned surface vehicle, rudderless double thrusters

I. Introduction

Unmanned Surface Vessels (USVs) are receiving great attention worldwide due to its practicality [1]. As a classic motion control method, path following controls a vehicle to follow a spatial path without any temporal constraints [2]. In the following, we briefly list some of the recent works related to the fault-tolerant control (FTC) for path following control of USVs. In [3], a nonlinear observer is proposed to get the total disturbance that includes the adverse effects of unknown disturbances, actuator saturation and faults. In [4], an observer is developed to obtain the information of actuator faults and states simultaneously for the surface vehicle with transmission delays and package loss during the network communication. In [5], an FTC strategy is designed by combining a normal control method with an additional fault estimating and cancelling approach. In [6], an adaptive fault-tolerant controller is designed by Backstepping method for the tracking control of USVs. Depending on how to work with redundancies, above FTC methods can be sorted into two classes, active FTC (AFTC) [5], and passive FTC (PFTC) [4]-[6]. The detailed discussion about these two methods can be found in [7]. In contrast to the PFTC, the AFTC system is made up by a fault detection and diagnosis (FDD) module offering faults size, a fault-tolerant controller cancelling the adverse effects caused by faults, and a decision mechanism determining when and how to put the reconfiguration controller into action [8]. Therefore, the AFTC strategy is more flexible and practical than PFTC strategy. Unfortunately, the AFTC strategy for path following control of the surface vehicle with rudderless double thrusters has not been proposed in the existing literatures, to the existing knowledge of the authors. Compared to the use of AFTC in USVs, AFTC is more common in spacecraft and aircraft [8]-[12]. Motivated by the above results, an AFTC method is proposed for path following control of a surface vehicle with rudderless double thrusters. The main contributions are as follows:

- The inputs saturation and gain faults of propellers are considered simultaneously. The fault detection and fault observer are designed to get fault information accurately. By using Lyapunov stability theorem, it is proved that all tracking errors are uniformly bounded.
- The AFTC strategy developed in this paper can precisely estimate the fault information of actuators, and provide corresponding compensation to ensure that the surface vehicle can accurately track the predefined path in case of partial gain loss of the actuator.

The rest of this paper is organized as follows. Section II formulates path following problem of the surface vehicle with inputs saturation and thruster faults. The AFTC strategy is developed in Section III. Simulation studies is conducted in Section IV. Conclusion is presented in Section V.

II Problem Formulation

A Surface Vessel Model

The simplified dynamics of the underactuated surface vehicle with double thrusters can be written as [13]:

$$\dot{x} = ucos(\psi) - vsin(\psi) \tag{1}$$

$$\dot{y} = usin(\psi) + vcos(\psi) \tag{2}$$

$$\dot{\psi} = r \tag{3}$$

$$\dot{v} = f_v + \Delta f_v + \tau_{w2}/m_{22} \tag{4}$$

$$\dot{\boldsymbol{\xi}} = \boldsymbol{F}(\boldsymbol{v}) + \boldsymbol{\Delta_F} + (\boldsymbol{B} + \boldsymbol{\Delta_B})\boldsymbol{T} + \boldsymbol{\xi_w} \tag{5}$$

where ψ denotes the yaw angle, u, v and r are the surge, sway and yaw angle velocities (see Fig.1), $\boldsymbol{\xi} = [u, r]^T$, $\boldsymbol{\Delta_F}$ and $\boldsymbol{\Delta_B}$ are unmodeled terms, $\boldsymbol{T} = [T_1, T_2]^{\mathrm{T}}$ is the control inputs vector, $\boldsymbol{\xi_w} = [\tau_{w1}/m_{11}, \tau_{w3}/m_{33}]^T$ is external disturbance, $f_v = -\frac{d_{22}}{m_{22}}v - \frac{m_{11}ur}{m_{22}}$, $\boldsymbol{F}(\boldsymbol{v})$ and $\boldsymbol{B}$ are given by:

$$\boldsymbol{F}(\boldsymbol{v}) = \begin{bmatrix} -\frac{d_{11}}{m_{11}}u + \frac{m_{22}vr}{m_{11}} \\ -\frac{d_{33}}{m_{33}}r + \frac{(m_{11}-m_{22})uv}{m_{33}} \end{bmatrix}, \boldsymbol{B} = \begin{bmatrix} \frac{1}{m_{11}} & \frac{1}{m_{11}} \\ \frac{d_p}{m_{33}} & -\frac{d_p}{m_{33}} \end{bmatrix}$$

where m_{ii}, $i = 1,2,3$ represent the vehicle inertia mass and the added mass, and d_p is the lateral distance from the centerline of the surface vehicle to the centerline of each actuator.

B. Actuator Saturation and Fault Models

It is assumed that the available thrust generate by the two propellers is limited by T_{max} and T_{min}. Due to the saturation nonlinearities of actuators, the saturated outputs of the USV can be described as follows：

$$\boldsymbol{T} = \boldsymbol{T_c} - \boldsymbol{\Delta_c} \tag{6}$$

where $\boldsymbol{\Delta_c} = \boldsymbol{T_c} - \mathrm{sat}(\boldsymbol{T_c})$, $\boldsymbol{T_c} = [T_{c1}, T_{c2}]$, which are all known perfectly. For the double thrusters fitted on catamarans, faults may occur in electronic circuits, drive motor, bearing of shafts and energy supply due to the lack of maintenance or other nuexpected conditions. The faults acting on the actuators of USV can be modelled as：

$$\boldsymbol{T_f} = (\boldsymbol{I_2} - \boldsymbol{E_2})\boldsymbol{T} \tag{7}$$

where the matrix $\mathbf{I_2} = \mathrm{diag}(1,1)$, $\boldsymbol{E_2} = \mathrm{diag}\{e_1, e_2\}$, which is unknown, represents the partial gain loss of the thrusters and the diagonal elements satisfy $0 \le e_i \le 1$. The term e_i can be given as $e_i = \frac{a_i}{1+\rho_i e^{-\vartheta_i(t)}}$, $i = 1,2$, where $a_i = 0$ or $a_i = 1$, and $\rho_i \ge 0$, $i = 1,2$, which are used to adjust the value e_i. It should be noted that $0 < e_i < 1$ $(a_i = 1, \rho_i > 0)$ implies the thruster partially occurs failure, $e_i = 0$ $(a_i = 0)$ implies the thruster is ideal, and $e_i = 1$ $(a_i = 1, \rho_i = 0)$ implies the thruster is totally failed. Let $\boldsymbol{H}(\boldsymbol{T}, t) = \boldsymbol{E_2}\boldsymbol{T}$, which is unknown. Replacing $\boldsymbol{T}$ in (5) with $\boldsymbol{T_f}$ in (7), the MIMO subsystem (5) can be rewritten as:

$$\dot{\boldsymbol{\xi}} = \boldsymbol{F}(\boldsymbol{v}) + \boldsymbol{BT} + \boldsymbol{\delta_d} + \boldsymbol{\delta_f} + \boldsymbol{\xi_w} \tag{8}$$

where $\boldsymbol{\delta_d} = [\boldsymbol{\Delta_F} + \boldsymbol{\Delta_B}(\boldsymbol{T} - \boldsymbol{H})]$, $\boldsymbol{\delta_f} = -\boldsymbol{BH}$, ($\boldsymbol{H}$ is the simplified form of $\boldsymbol{H}(\boldsymbol{T}, t)$), substituting (6) into (8), we have

$$\dot{\boldsymbol{\xi}} = \boldsymbol{F}(\boldsymbol{v}) + \boldsymbol{BT_c} - \boldsymbol{B\Delta_c} + \boldsymbol{\delta_f} + \boldsymbol{\xi_w} + \boldsymbol{\delta_d} \tag{9}$$

Assumption 1. There exists a positive constant d_1 satisfying that $\|(\boldsymbol{\delta_d^T}, \boldsymbol{\xi_w^T})\| \le d_1$.

Assumption 2. There exists a positive constant d_2 satisfying that $\|\dot{\boldsymbol{\delta}}_{\boldsymbol{f}}\| \le d_2$.

Remark 1. The energy of environment disturbances and control inputs are limited, so that Assumption 1 is reasonable. Since the derivatives of $\boldsymbol{E_2}$ and $\boldsymbol{T}$ are both bounded, the $\|\dot{\boldsymbol{\delta}}_{\boldsymbol{f}}\|$ is also bounded, so that the Assumption 2 is reasonable.

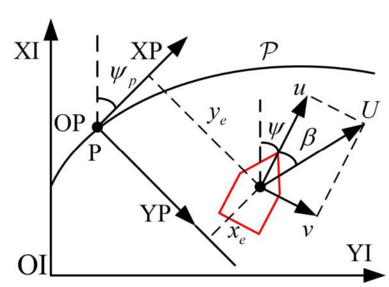

Fig.1. Geometrical illustration of vessel guidance.

C. Control Objective

The following task is to establish path-following error dynamics as illustrated in Fig.1. We parameterize the desired path $\mathcal{P}$ using a time varying variable θ. Furthermore, for every point $\mathrm{P} = (x_p(\theta), y_p(\theta))$ located on the path, i.e., $\mathrm{P} \in \mathcal{P}$, we establish a path tangential frame {P}:XP-OP-YP as shown in Fig.1. Then, the path-following errors can be represented by the vehicle position in the frame {P} denoted by $\boldsymbol{P_e} = [x_e, y_e]^T$, which can be calculated by

$$\begin{bmatrix} x_e \\ y_e \end{bmatrix} = \begin{bmatrix} cos(\psi_p) & sin(\psi_p) \\ -sin(\psi_p) & cos(\psi_p) \end{bmatrix} \begin{bmatrix} x - x_p(\theta) \\ y - y_p(\theta) \end{bmatrix} \tag{10}$$

where ψ_p is the angle of parameterized path $\mathcal{P}$ at point P with respect to inertial XI-axis, $\psi_p = \mathrm{atan2}(y_p'(\theta), x_p'(\theta))$. The error dynamics can be calculated by substituting (1) and (2) in the derivative of (10), which is given by

$$\dot{x}_e = ucos(\psi_e) - vsin(\psi_e) + k_c u_p y_e - u_p \tag{11}$$

$$\dot{y}_e = usin(\psi_e) + vcos(\psi_e) - k_c u_p x_e \tag{12}$$

where $\psi_e = \psi - \psi_p$. Note that $\dot{\psi}_p = k_c u_p$, where u_p is the speed of point P, which can be calculated by $u_p = \dot{\theta}\sqrt{(x_{\mathrm{p}}')^2 + (y_{\mathrm{p}}')^2}$, k_c is the curvature of path $\mathcal{P}$ at the point P.

Control Objective: If all the states of the surface vehicle can be obtained perfectly, the control objective of AFTC for curved path following is to force vehicle to track the given path $\mathcal{P}$ under the model uncertainties, external interferences and partial gain loss of thrusters. The tracking errors defined in (10) satisfy that $\lim_{t\to\infty}\|(x_e, y_e)\| \le d_3$, where $d_3 > 0$, and all errors in the closed-loop system are bounded.

III. Control Design

This section aims to develop an AFTC scheme for curved path following control of USV under the external interferences and thruster faults. Fig.2 shows the global framework of the AFTC strategy developed in this paper. The FDD scheme consists of fault detection and fault estimation, which are employed to detect the existence of gain loss and obtain the size of the gain loss. The fault-tolerant controller is designed based on the fault estimated value from FDD to cancel the adverse effects of partial gain loss of thrusters and guarantee the control performance. In this section, the FDD scheme and fault-tolerant controller are proposed.

A. Fault Detection

To get the time of failure, fault detection approach is developed in this subsection. Based on the surge and yaw motion dynamics in (8), the fault detection observer can be designed as:

$$\dot{\widehat{\boldsymbol{D}}} = \boldsymbol{F}(\boldsymbol{\nu}) + \boldsymbol{BT} + \boldsymbol{L}(\boldsymbol{\xi} - \widehat{\boldsymbol{D}}) \tag{13}$$

where $\widehat{\boldsymbol{D}}$ is the estimate value of $\boldsymbol{\xi}$. Define estimate error $\widetilde{\boldsymbol{D}} = \boldsymbol{\xi} - \widehat{\boldsymbol{D}}$, combining (8) and (13), we can get

$$\dot{\widetilde{\boldsymbol{D}}} = -\boldsymbol{L}\widetilde{\boldsymbol{D}} + \boldsymbol{\delta_f} + \boldsymbol{\xi_w} + \boldsymbol{\delta_d} \tag{14}$$

The policy decision for gain loss detection of thrusters is concluded in the following theorem.

Theorem 1. The decision on the event of actuator faults is made when the estimation error $\|\widetilde{\boldsymbol{D}}\|$ given in (14) exceeds the predefined threshold given by $D_{th} = \frac{\bar{\xi}_{\mathrm{w}} + \bar{\delta}_{\mathrm{d}}}{\lambda_{min}(L)}$, where $\bar{\xi}_{\mathrm{w}}$ and $\bar{\delta}_{\mathrm{d}}$ represent the upper bounds of $\|\boldsymbol{\xi_w}\|$ and $\|\boldsymbol{\delta_d}\|$ respectively.

Proof: Consider a Lyapunov function as $V_{o1} = 0.5\widetilde{\boldsymbol{D}}^T\widetilde{\boldsymbol{D}}$, the derivative of $\mathrm{V_{o1}}$ along (14) is given as

$$\begin{aligned} \dot{V}_{o1} &= \widetilde{\boldsymbol{D}}^T(-\boldsymbol{L}\,\widetilde{\boldsymbol{D}} + \boldsymbol{\delta_f} + \boldsymbol{\xi_w} + \boldsymbol{\delta_d}) \\ &\le -\lambda_{min}(\boldsymbol{L})\|\widetilde{\boldsymbol{D}}\|^2 + \bar{d}_1\|\widetilde{\boldsymbol{D}}\| + \bar{\delta}_f\|\widetilde{\boldsymbol{D}}\| \end{aligned} \tag{15}$$

where $\bar{d}_1$ is given in Assumption 1. The notation $\lambda_{min}[*]$ represents the minimum eigenvalue of matrix $*$. If there are no faults in the propellers, i.e., the total faults effect satisfies $\boldsymbol{\delta_f} = 0$, the foregoing inequality becomes

$$\dot{V}_{o1} \le -\lambda_{min}(\boldsymbol{L})\|\widetilde{\boldsymbol{D}}\|^2 + \bar{d}_1\|\widetilde{\boldsymbol{D}}\| \tag{16}$$

It is clear that $\dot{V}_{o1} < 0$ if $\|\widetilde{\boldsymbol{D}}\| > D_{th}$, supposing that the initial value of the detection observer given in (13) is set to satisfy $||\widetilde{\boldsymbol{D}}(0)|| \le D_{th}$, then, the estimate error will satisfy $||\widetilde{\boldsymbol{D}}|| \le D_{th}$ forever, which implies that the error $||\widetilde{\boldsymbol{D}}||$ is upper bounded by a constant D_{th}, if there exists a time interval Ξ satisfying that $\|\widetilde{\boldsymbol{D}}\| > D_{th}$ for $t \in \Xi$, it means that $\boldsymbol{\delta_f} > \boldsymbol{0}$ for $t \in \Xi$, i.e., the faults occur at this time interval. ■

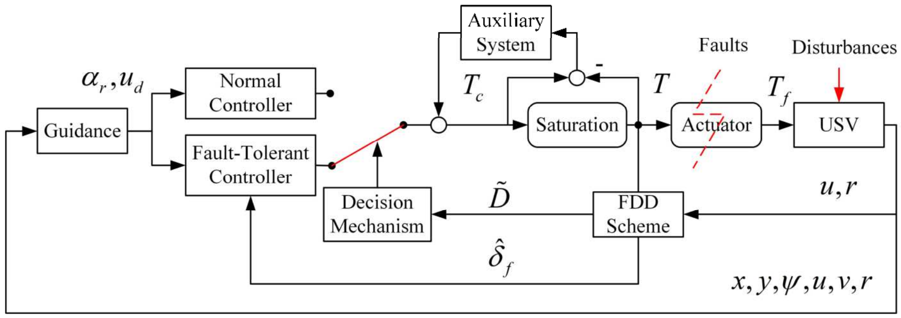

Fig.2. Structure of the proposed AFTC system

B. Fault Estimation

Followed by the fault detection, we need to estimate the size of gain loss in this part. To identify the thruster fault accurately in (8), an indirect fault estimation method is developed. First, an auxiliary variable borrowed from [12] is given as follows:

$$\boldsymbol{Q} = \boldsymbol{\delta_f} - \boldsymbol{\Lambda_1}\boldsymbol{\xi} \tag{17}$$

where $\boldsymbol{\Lambda_1} > \boldsymbol{0}$ is a positive matrix designed later. Taking the derivative of $\boldsymbol{Q}$ along (8), we can get the following result.

$$\dot{\boldsymbol{Q}} = \dot{\boldsymbol{\delta}}_{\boldsymbol{f}} - \boldsymbol{\Lambda_1}(\boldsymbol{F}(\boldsymbol{\nu}) + \boldsymbol{BT} + \boldsymbol{Q} + \boldsymbol{\Lambda_1}\boldsymbol{\xi} + \boldsymbol{\xi_w} + \boldsymbol{\delta_d}) \tag{18}$$

Let $\widehat{\boldsymbol{Q}}$ and $\widehat{\boldsymbol{\delta}}_{\boldsymbol{f}}$ be the estimated value of $\boldsymbol{Q}$ and $\boldsymbol{\delta_f}$. The indirect fault observer of thrusters can be designed as:

$$\dot{\widehat{\boldsymbol{Q}}} = -\boldsymbol{\Lambda_1}\widehat{\boldsymbol{Q}} - \boldsymbol{\Lambda_1}(\boldsymbol{F}(\boldsymbol{\nu}) + \boldsymbol{BT} + \boldsymbol{\Lambda_1}\hat{\boldsymbol{\xi}}) \tag{19}$$

$$\dot{\hat{\boldsymbol{\xi}}} = \boldsymbol{F}(\boldsymbol{\nu}) + \boldsymbol{BT} + \widehat{\boldsymbol{\delta}}_{\boldsymbol{f}} + \boldsymbol{\Lambda_2}(\boldsymbol{\xi} - \hat{\boldsymbol{\xi}}) \tag{20}$$

$$\widehat{\boldsymbol{\delta}}_{\boldsymbol{f}} = \widehat{\boldsymbol{Q}} + \boldsymbol{\Lambda_1}\hat{\boldsymbol{\xi}} \tag{21}$$

Define $\widetilde{\boldsymbol{Q}} = \boldsymbol{Q} - \widehat{\boldsymbol{Q}}$, $\tilde{\boldsymbol{\xi}} = \boldsymbol{\xi} - \hat{\boldsymbol{\xi}}$, $\widetilde{\boldsymbol{\delta}}_{\boldsymbol{f}} = \boldsymbol{\delta_f} - \widehat{\boldsymbol{\delta}}_{\boldsymbol{f}}$, respectively. The error dynamics are derived as follows:

$$\dot{\widetilde{\boldsymbol{Q}}} = -\boldsymbol{\Lambda_1}\widetilde{\boldsymbol{Q}} - \boldsymbol{\Lambda_1^2}\tilde{\boldsymbol{\xi}} + \dot{\boldsymbol{\delta}}_{\boldsymbol{f}} - \boldsymbol{\Lambda_1}(\boldsymbol{\xi_w} + \boldsymbol{\delta_d}) \tag{22}$$

$$\dot{\tilde{\boldsymbol{\xi}}} = -\boldsymbol{\Lambda_2}\tilde{\boldsymbol{\xi}} + \widetilde{\boldsymbol{Q}} + \boldsymbol{\Lambda_1}\tilde{\boldsymbol{\xi}} + \boldsymbol{\xi_w} + \boldsymbol{\delta_d} \tag{23}$$

$$\widetilde{\boldsymbol{\delta}}_{\boldsymbol{f}} = \widetilde{\boldsymbol{Q}} + \boldsymbol{\Lambda_1}\tilde{\boldsymbol{\xi}} \tag{24}$$

Base on the derived fault error dynamics (22)-(24), the result for fault estimator is obtained as the following theorem.

Theorem 2. Considering the fault errors dynamics (22)-(24) with the Assumption 1, for the given constants $\gamma > 0$ and $\varepsilon > 0$, if there exist matrixes $\boldsymbol{\Lambda_1} > \boldsymbol{0}$ and $\boldsymbol{\Lambda_2} > \boldsymbol{0}$ such that the inequality given in (25) holds.

$$\begin{bmatrix} \boldsymbol{\Lambda_2} - \boldsymbol{\Lambda_1} - \varepsilon\boldsymbol{I_2} & \frac{1}{2}(\frac{\boldsymbol{\Lambda_1^2}}{\gamma} - \boldsymbol{I_2}) \\ (\Lambda_1^2/\gamma - \boldsymbol{I_2})/2 & \frac{1}{\gamma}(\boldsymbol{\Lambda_1} - \frac{\boldsymbol{\Lambda_1}\boldsymbol{\Lambda_1^T}}{\varepsilon} - \frac{\boldsymbol{I_2}}{2\varepsilon}) \end{bmatrix} > 0 \tag{25}$$

Then the faults estimator proposed in (19), (20) and (21) guarantees that the faults estimation error $\widetilde{\boldsymbol{\delta}}_{\boldsymbol{f}}$ exponentially converges to a compact set including the origin.

Proof: Construct Lyapunov candidate as follows $V_{o2} = 0.5\widetilde{\boldsymbol{Q}}^T\widetilde{\boldsymbol{Q}}/\gamma + 0.5\tilde{\boldsymbol{\xi}}^T\tilde{\boldsymbol{\xi}}$. The time derivative V_{o2} along with (22), (23) and (24) is given as:

$$\begin{aligned}\dot{V}_{o2} \le & -\widetilde{\boldsymbol{Q}}^T\frac{1}{\gamma}\left(\boldsymbol{\Lambda_1} - \frac{\boldsymbol{\Lambda_1}\boldsymbol{\Lambda_1^T}}{\varepsilon} - \frac{\boldsymbol{I_2}}{2\varepsilon}\right)\widetilde{\boldsymbol{Q}} - \tilde{\boldsymbol{\xi}}^T(\boldsymbol{\Lambda_2} - \boldsymbol{\Lambda_1} - \varepsilon\boldsymbol{I_2})\tilde{\boldsymbol{\xi}} - \\ & \widetilde{\boldsymbol{Q}}^T\left(\frac{\boldsymbol{\Lambda_1^2}}{\gamma} - \boldsymbol{I_2}\right)\tilde{\boldsymbol{\xi}} + \frac{\varepsilon}{2\gamma}\bar{\dot{\delta}}_f + \left(\frac{1}{2\varepsilon} + \frac{\varepsilon}{2\gamma}\right)(\bar{\xi}_w + \bar{\delta}_d) \\ \le & -[\widetilde{\boldsymbol{Q}}^T \quad \tilde{\boldsymbol{\xi}}^T]\boldsymbol{P_1}[\widetilde{\boldsymbol{Q}}^T \quad \tilde{\boldsymbol{\xi}}^T]^T + \sigma_1 \end{aligned} \tag{26}$$

where $\varepsilon > 0$, $\boldsymbol{P_1}$ is given in (25), and $\sigma = \frac{\varepsilon}{2\gamma}d_2 + \left(\frac{1}{2\varepsilon} + \frac{\varepsilon}{2\gamma}\right)d_1$. If the matrix $\boldsymbol{P_1}$ is positive definite, we have

$$\dot{V}_{o1} \le -\kappa_1 V_{o1} + \sigma_1 \tag{27}$$

where $\kappa_1 = \frac{2\lambda_{min}(\boldsymbol{P_1})}{\max(1, 1/\gamma)}$. According Lyapunov stability theory, we can easily obtain that the estimate errors $\widetilde{\boldsymbol{Q}}$ and $\tilde{\boldsymbol{\xi}}$ are uniformly bounded. Define the invariant set $\Omega_{(\widetilde{Q},\tilde{\xi})}$ as

$$\Omega_{(\widetilde{Q},\tilde{\xi})} = \{(\widetilde{\boldsymbol{Q}}, \tilde{\boldsymbol{\xi}}) | \frac{1}{2\gamma}\|\widetilde{\boldsymbol{Q}}\|^2 + \frac{1}{2}\|\tilde{\boldsymbol{\xi}}\|^2 \le \frac{\sigma_1}{\kappa_1}\} \tag{28}$$

The supplementary set of $\Omega_{(\widetilde{Q},\tilde{\xi})}$ is denoted by $\bar{\Omega}_{(\widetilde{Q},\tilde{\xi})}$. Considering (27), we can get that $\dot{V}_{o1} < 0$ if $(\widetilde{\boldsymbol{Q}}, \tilde{\boldsymbol{\xi}}) \in \bar{\Omega}_{(\widetilde{Q},\tilde{\xi})}$. Therefore, it is clear that $(\widetilde{\boldsymbol{Q}}, \tilde{\boldsymbol{\xi}})$ converges to the invariant set $\Omega_{(\widetilde{Q},\tilde{\xi})}$ exponentially. According to (24), it can be noted that $\widetilde{\boldsymbol{\delta}}_{\boldsymbol{f}}$

is a combination of $\widetilde{\boldsymbol{Q}}$ and $\tilde{\boldsymbol{\xi}}$. Therefore, we can conclude that the faults estimate error $\widetilde{\boldsymbol{\delta}}_{\boldsymbol{f}}$ will converge to a compact set including the origin exponentially. ■

C. Fault Tolerant Controller

In this subsection, the fault-tolerant controller based on the estimated value of gain loss is developed to cancel the adverse effects of gain loss and recover the system performance of path following if faults occur in the thrusters.

Step 1. Define the tracking errors of course angle and velocities as $\tilde{\psi} = \psi - \psi_d$, $\tilde{u} = u - u_d$. Then, the error dynamics in (12) can be rewritten as:

$$\dot{x}_e = U_d cos(\chi_P) + k_c u_p y_e + \tilde{u} cos(\psi_e) - u_p \tag{29}$$

$$\dot{y}_e = U_d sin(\chi_p^d) + U_d w \tilde{\psi} + \tilde{u} sin(\psi_e) - k_c u_p x_e \tag{30}$$

where $\chi_p = \psi + \beta_d - \psi_p$, $\chi_p^d = \psi_d + \beta_d - \psi_p$, $U_d = \sqrt{u_d^2 + v^2}$, $\mathrm{w} = w_1 \sin(\chi_p^d) + w_2 \cos(\chi_p^d)$, where $\beta_d = \arctan(v/u_d)$, $w_1 = (\cos(\tilde{\psi}) - 1)/\tilde{\psi}$, $w_2 = \sin(\tilde{\psi})/\tilde{\psi}$. We can easily get $|w|$ is bounded, $|w| < 1.73$. To stabilize x_e and y_e, the LOS guidance law ψ_d and u_p can be chosen as

$$\psi_d = \psi_p - acrtan\left(\frac{y_e}{\Delta}\right) - \beta_d \tag{31}$$

$$u_p = U_d cos(\chi_P) + \tilde{u} cos(\psi_e) + k_1 x_e \tag{32}$$

where $k_1 > 0$, $\Delta > 0$. According to (31), we can easily get, $\sin(\chi_p^d) = -\frac{y_e}{\sqrt{y_e^2+\Delta^2}}$, $\cos(\chi_p^d) = \frac{\Delta}{\sqrt{y_e^2+\Delta^2}}$. Substituting (31) and (32) into (29) and (30) respectively, we can get:

$$\dot{x}_e = -k_1 x_e + k_c u_p y_e \tag{33}$$

$$\dot{y}_e = -\phi y_e + U_d w \tilde{\psi} + \tilde{u} sin(\psi_e) - k_c u_p x_e \tag{34}$$

where $\phi = \frac{U_d}{\sqrt{y_e^2+\Delta^2}} > 0$. Now, we construct Lyapunov candidate as $V_1 = 0.5x_e^2 + 0.5y_e^2$, the derivative of V_1 along with (33) and (34) is given as

$$\dot{V}_1 = -k_1 x_e^2 - \phi y_e^2 + U_d w \tilde{\psi} y_e - \tilde{u} sin(\psi_e) y_e \tag{35}$$

Step 2. Define the tracking error $\tilde{r} = r - \alpha_r$, where α_r is virtual law designed later. The derivative of $\tilde{\psi}$ can be given

$$\dot{\tilde{\psi}} = \tilde{r} + \alpha_r - \dot{\psi}_d \tag{36}$$

where $\dot{\psi}_d = k_c u_p - u_d \dot{v}/U_d^2 - \dot{y}_e \phi \Delta / U_d$. Then, the virtual control law α_r can be designed as follows:

$$\alpha_r = \dot{\psi}_d - k_2 \tilde{\psi} \tag{37}$$

where $\mathrm{k}_2 > 0$. Substituting (37) into (36), we can get $\dot{\tilde{\psi}} = \tilde{r} - k_2 \tilde{\psi}$. Then, we construct the second Lyapunov candidate as $V_2 = V_1 + 0.5\tilde{\psi}^2$. The derivative of V_2 is calculated by

$$\dot{V}_2 = \dot{V}_1 - k_2 \tilde{\psi}^2 + \tilde{r}\tilde{\psi} \tag{38}$$

Step 3. Considering the actuator saturation, we can adopt the 1-st order auxiliary systems as follows

$$\dot{\boldsymbol{\lambda}} = -\boldsymbol{A\lambda} - \boldsymbol{B\Delta_c} \tag{39}$$

Let $\boldsymbol{\xi_d} = [u_d, \alpha_r]^T$, $\tilde{\boldsymbol{\xi}} = \boldsymbol{\xi} - \boldsymbol{\xi_d} - \boldsymbol{\lambda}$, combining (9) and (39), the derivative of $\tilde{\xi}$ can be get as follows:

$$\dot{\tilde{\boldsymbol{\xi}}} = \boldsymbol{F(v)} + \boldsymbol{BT_c} + \boldsymbol{A\lambda} + \boldsymbol{\delta_f} + \boldsymbol{\xi_w} + \boldsymbol{\delta_d} - \dot{\boldsymbol{\xi}}_{\boldsymbol{d}} \tag{40}$$

To refrain from the complicated calculations of $\dot{\boldsymbol{\xi}}_{\boldsymbol{d}}$, the following 1-st order filter is introduced: $\boldsymbol{T_1}\dot{\boldsymbol{\xi}}_{\boldsymbol{df}} + \boldsymbol{\xi_{df}} = \boldsymbol{\xi_d}$, where $\boldsymbol{\xi_{df}}$ is the filtered value of $\boldsymbol{\xi_d}$. The filtered error is defined as $\tilde{\boldsymbol{\xi}}_{\boldsymbol{f}} = \boldsymbol{\xi_{df}} - \boldsymbol{\xi_d}$, its derivative can be obtained as:

$$\dot{\tilde{\boldsymbol{\xi}}}_f = -T_1^{-1}\tilde{\boldsymbol{\xi}}_f - \dot{\boldsymbol{\xi}}_{\boldsymbol{d}} \tag{41}$$

Let $\boldsymbol{S} = [0, \tilde{\psi}]^T$, then, the control law can be given as:

$$\boldsymbol{T_c} = \boldsymbol{B}^{-1}(-\boldsymbol{F} - \boldsymbol{G}\tilde{\boldsymbol{\xi}} - \overline{\boldsymbol{d}} sgn(\tilde{\boldsymbol{\xi}}) - \boldsymbol{A\lambda} - \widehat{\boldsymbol{\delta}}_{\boldsymbol{f}}' + \dot{\boldsymbol{\xi}}_{\boldsymbol{df}} - \boldsymbol{S}) \tag{42}$$

where $\boldsymbol{G} > 0$, $\overline{\boldsymbol{d}} > 0$, $\widehat{\boldsymbol{\delta}}_{\boldsymbol{f}}' = k_3 \widehat{\boldsymbol{\delta}}_{\boldsymbol{f}}$, $k_3 = 1$ or $k_3 = 0$, the meaning of k_3 is explained later. Substituting (42) into (40), we can get:

$$\dot{\tilde{\boldsymbol{\xi}}} = -\boldsymbol{G}\tilde{\boldsymbol{\xi}} - \overline{\boldsymbol{d}} sgn(\tilde{\boldsymbol{\xi}}) + e_\delta + \boldsymbol{\xi_w} + \boldsymbol{\delta_d} - \dot{\boldsymbol{\xi}}_{\boldsymbol{d}} \tag{43}$$

where $\mathrm{e}_\delta = \boldsymbol{\delta_f} - \widehat{\boldsymbol{\delta}}_{\boldsymbol{f}}'$, and $\overline{\boldsymbol{d}} > 0$. Then, we construct the third Lyapunov candidate as follows:

$$V_3 = V_2 + 0.5\tilde{\boldsymbol{\xi}}^T\tilde{\boldsymbol{\xi}} + 0.5\tilde{\boldsymbol{\xi}}_f^T\tilde{\boldsymbol{\xi}}_f + 0.5\boldsymbol{\lambda}^T\boldsymbol{\lambda} \tag{44}$$

The derivative of V_3 along with (39), (40) is given by

$$\begin{aligned}\dot{V}_3 = \dot{V}_1 - k_2\tilde{\psi}^2 - \tilde{\boldsymbol{\xi}}^T\boldsymbol{G}\tilde{\boldsymbol{\xi}} - \tilde{\boldsymbol{\xi}}_f^T\boldsymbol{T}^{-1}\tilde{\boldsymbol{\xi}}_f - \boldsymbol{\lambda}^T\boldsymbol{A\lambda} - \\ \tilde{\boldsymbol{\xi}}^T\overline{\boldsymbol{d}} sgn(\tilde{\boldsymbol{\xi}}) + \tilde{\boldsymbol{\xi}}^T(\boldsymbol{\xi_w} + \boldsymbol{\delta_d}) - \boldsymbol{\lambda}^T\boldsymbol{B\Delta_c} - \\ \tilde{\boldsymbol{\xi}}_f^T\dot{\boldsymbol{\xi}}_{\boldsymbol{d}} - \tilde{\boldsymbol{\xi}}^T\dot{\boldsymbol{\xi}}_{\boldsymbol{d}} + \tilde{\boldsymbol{\xi}}^T\boldsymbol{e_\delta}\end{aligned} \tag{45}$$

Remark 2. The normal controller can be written as $\boldsymbol{T_c} = \boldsymbol{B}^{-1}(-\boldsymbol{F} - \boldsymbol{G}\tilde{\boldsymbol{\xi}} - \bar{\boldsymbol{d}}\mathrm{sgn}(\tilde{\boldsymbol{\xi}}) - \boldsymbol{A}\boldsymbol{\lambda} + \dot{\boldsymbol{\xi}}_{\boldsymbol{df}} - \boldsymbol{S})$, the only difference from (42) is no fault compensation term $\widehat{\boldsymbol{\delta}}'_{\boldsymbol{f}}$. The workflow of the proposed AFTC strategy in Fig.2 can be described as: Guidance system is used to produce the virtual control law α_r and u_d, and FDD scheme detect the failure at all times, if the faults occur, i.e., $\|\widetilde{\boldsymbol{D}}\| > D_{th}$, then, the fault estimation starts working. If the fault detection error and fault estimation error satisfy the condition, $\|\widetilde{\boldsymbol{D}}\| > D_{th}$ and $\|\widetilde{\boldsymbol{H}}\| < H_{th}$ where $\widetilde{\boldsymbol{H}} = \boldsymbol{B}^{-1}\widetilde{\boldsymbol{\delta}}_{\boldsymbol{f}}$, then, the normal controller will be switched to fault-tolerant controller (42) to accommodate actuator faults, $k_3 = 1$, otherwise, $k_3 = 0$.

D Main Result

Theorem 3. Consider the USV dynamics given in (1)-(5) with actuator inputs saturation modelled in (6) and gain faults modelled in (7). If the fault-tolerant controller designed in (42) with the guidance law (31), virtual target speed assignment law (31), virtual control law (37) and auxiliary system (39) are employed with the effective fault identification and estimation, then the closed-loop system is uniformly ultimately bounded stable, and all tracking errors will converge to a small neighborhood of the origin even if the gain loss occur.

Proof: If the estimation error $\|\widetilde{\boldsymbol{D}}\| > D_{th}$ in fault detection, the fault tolerant controller developed in (42) will be applied. According to (45) and assuming $\lambda_{min}\{\bar{\boldsymbol{d}}\} > d_1$, we have

$$\dot{V}_3 \leq -k_1 x_e^2 - l_{ye} y_e^2 - l_{\tilde{\psi}}\tilde{\psi}^2 - \tilde{\boldsymbol{\xi}}^T P_{\tilde{\xi}}\tilde{\boldsymbol{\xi}} - \tilde{\boldsymbol{\xi}}_{\boldsymbol{f}}^{\boldsymbol{T}} \boldsymbol{P}_{\xi_f}\tilde{\boldsymbol{\xi}}_{\boldsymbol{f}} - \boldsymbol{\lambda}^T P_\lambda \boldsymbol{\lambda} + \sigma_2 \quad (46)$$

where $l_{ye} = \left(\phi - \frac{1}{\varepsilon} - U_d\frac{\varepsilon w^2}{2}\right)$, $l_{\tilde{\psi}} = \left(k_2 - \frac{1}{2\varepsilon}\right)$, $\boldsymbol{P}_{\tilde{\xi}} = \left(\boldsymbol{G} - \frac{3}{2\varepsilon}\boldsymbol{I_2}\right)$, $\boldsymbol{P}_{\xi_f} = \left(\boldsymbol{T}_2^{-1} - \frac{1}{2\varepsilon}\boldsymbol{I_2}\right)$, $\boldsymbol{P_\lambda} = \left(\boldsymbol{A} - \frac{1}{2\varepsilon}\boldsymbol{I_2}\right)$, $\sigma_2 = \varepsilon\left\|\dot{\boldsymbol{\xi}}_{\boldsymbol{d}}\right\|^2 + \frac{\varepsilon}{2}\|\boldsymbol{B}\boldsymbol{\Delta_c}\|^2 + \frac{\varepsilon}{2}\|\boldsymbol{e_\delta}\|^2$, $\varepsilon > 0$. It should be noted that σ_2 is bounded. We can choose appropriate parameters such that $l_{ye} > 0$, $l_{\tilde{\psi}} > 0$, $\boldsymbol{P}_{\tilde{\xi}} > 0$, $\boldsymbol{P}_{\xi_f} > \boldsymbol{0}$, $\boldsymbol{P}_\lambda > 0$, then (46) can be rewrite as follows

$$\dot{V}_3 \leq -\kappa_2 V_3 + \sigma_2 \quad (47)$$

where $\kappa_2 = 2\min\{k_1, \mathrm{l_{ye}}, l_{\tilde{\psi}}, \lambda\{\boldsymbol{P}_{\tilde{\xi}}\}, \lambda_{min}\left\{\boldsymbol{P}_{\xi_f}\right\}, \lambda_{min}(\boldsymbol{P_\lambda})\}$, According to Lyapunov stability theory, it can be concluded that all errors, x_e, y_e, $\tilde{\chi}_{sf}$, $\tilde{x}_1$, $\tilde{\boldsymbol{\xi}}$, $\tilde{\boldsymbol{x}}_{\boldsymbol{2}}$ and $\boldsymbol{\lambda}$ are uniformly bounded. If the estimation error $\|\widetilde{\boldsymbol{D}}\| \leq D_{th}$ in fault detection, there is $\boldsymbol{e_\delta} = \boldsymbol{0}$, $\sigma_2 = \varepsilon\left\|\dot{\boldsymbol{\xi}}_{\boldsymbol{d}}\right\|^2 + \frac{\varepsilon}{2}\|\boldsymbol{B}\boldsymbol{\Delta_c}\|^2$, it does not affect the system stability. This completes the proof. ∎

IV. SIMULATIONS

The simulation results of the proposed AFTC strategy for curved path following are presented in this section. The USV model is given in [13], the important parameters are as $m_{11} = 50.05$ kg, $m_{22} = 84.36$ kg, $m_{33} = 17.21$ kg, $d_{11} = 151.57$ kg/s, $d_{22} = 132.5$ kg/s, $d_{33} = 34.56$ kg/s, $d_p = 0.26$ kgm. In this simulation, the desired path is chosen as $x_p = 10\cos(\theta) + 11$, $y_p = 10\sin(\theta) + 11$, and the desired speed is $u_d = 0.6$ m/s, the initial state of USV is $x_0 = 8$ m, $y_0 = 2$ m, $\psi_0 = 30°$, $u_0 = v_0 = 0$ m/s, $r_0 = 0$ rad/s. The disturbances and mode uncertainties are chosen as:

$$\boldsymbol{\tau_w} = \begin{bmatrix} 1.2 + 0.8\sin(0.5t)\cos(t) \\ 1.5 + 0.5\sin(0.5t)\cos(t) \\ 0.8 + 0.5\sin(0.5t)\cos(t) \end{bmatrix}, \boldsymbol{\Delta_B} = 0.01\boldsymbol{B}$$

The parameters of AFTC system can be chosen as $\boldsymbol{L} = \mathrm{diag}(40,40)$, $\boldsymbol{\Lambda_1} = \mathrm{diag}(5,5)$, $\boldsymbol{\Lambda_2} = \mathrm{diag}(20,20)$, $k_1 = 3$, $\Delta = 2\,m$, $k_2 = 0.8$, $\boldsymbol{G} = \mathrm{diag}(1,1)$, $\boldsymbol{T_1} = \mathrm{diag}(0.1, 0.1)$, $\boldsymbol{A} = \mathrm{diag}(50,50)$, and the threshold of fault detection and estimation $D_{th} = 0.005$, $H_{th} = 6$. The fault scenario in this experiment is that the two propellers suffer the varying degrees of gain loss during $15\mathrm{s} \leq t < 35\mathrm{s}$ with $a_1 = a_2 = 1$, $\rho_1 = \rho_2 = 1$, $\vartheta_1 = \vartheta_2 = 0$, $35\mathrm{s} \leq t < 55\mathrm{s}$ with $a_1 = a_2 = 1$, $\rho_1 = 1$, $\rho_2 = 99$, $\vartheta_1 = \vartheta_2 = 0$, and $55\mathrm{s} \leq t < 75\mathrm{s}$ with $a_1 = a_2 = 1$, $\rho_1 = 99$, $\rho_2 = 1$, $\vartheta_1 = 0.05\sin(0.8t)$, $\vartheta_1 = 0.05\cos(0.8t)$. The simulation results are demonstrated in Fig.3~Fig.8. As illustrated in Fig.3~Fig.5 the fault detection and fault estimation strategy can obtain fault information accurately under the disturbances and model uncertainties. The fault tolerant controller outputs are illustrated in Fig.6. It can be clearly noted that the controller with AFTC can compensate unknown faults perfectly during 35s~75s compared to the controller without AFTC. As illustrated in Fig.7 and Fig.8, USV can track the predefined path and surge speed perfectly with AFTC strategy. As shown in Fig.8, all tracking errors converge to a vicinity of zero ultimately.

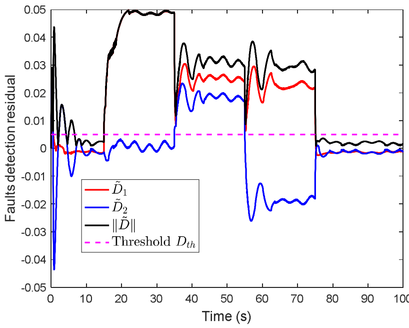

Fig.3. Faults detection

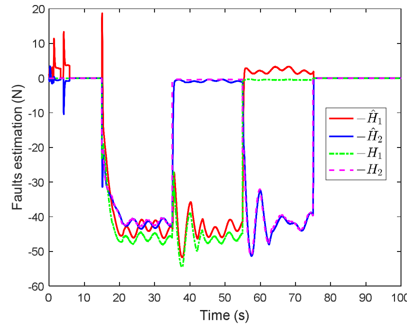

Fig.4. Faults estimation

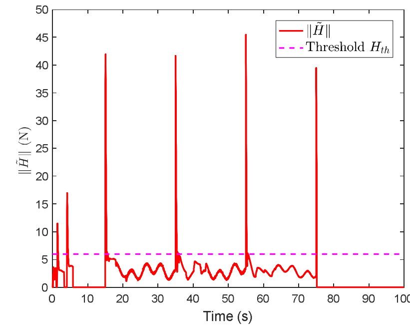

Fig.5. Faults estimation error

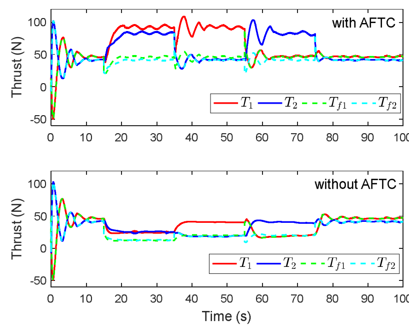

Fig.6. Thrust with AFTC and without AFTC

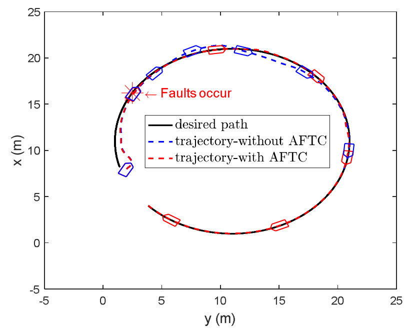

Fig.7. Desired path and trajectories

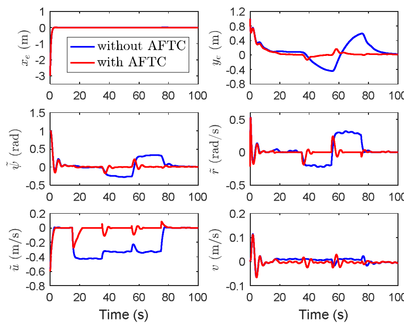

Fig.8. Tracking errors

V. Conclusion

In this paper, an AFTC scheme is proposed for path following control of USV with rudderless double thrusters suffering from actuator fault and inputs saturation. All errors of the AFTC system are validated to be bounded. In addition, the comparison simulation experiments have shown that the effectiveness of the developed AFTC strategy. Based on the proposed control scheme, the USV can accurately track the desired path under unknown external disturbances, actuator faults and input constraints.

Reference

[1]. Zhao, B., Zhang, X., Liang, C., and Han, "An Improved Model Predictive Control for Path-Following of USV Based on Global Course Constraint and Event-Triggered Mechanism," IEEE Access, vol. 9, pp 79725-79734, 2021.

[2]. G. Zhang and X. Zhang, "Practical robust neural path following control for underactuated marine vessels with actuators uncertainties," Asian J. Control, vol. 19, no. 1, pp. 173–187, 2017.

[3]. Zewei Zheng, Liang Sun, and Lihua Xie, "Error-Constrained LOS Path Following of a Surface Vessel with Actuator Saturation and Faults," IEEE T SYST MAN CY-S, 2017.

[4]. Zitian Zhou, Maiying Zhong, and Youqing Wang, "Fault Diagnosis Observer and Fault-Tolerant Control Design for Unmanned Surface Vehicles in Network Environments," IEEE Access, vol. 7, pp 173694-173702, 2019.

[5]. Zhixiang Liu, Youmin Zhang, and Chi Yuan, "Active Fault Tolerant Control of an Unmanned Surface Vehicle," 15th International Conference on Control, Automation and Systems (ICCAS 2015), 2015

[6]. Hongde Qin, Chengpeng Li, and Yanchao Sun, "Adaptive neural network-based fault-tolerant trajectory-tracking control of unmanned surface vessels with input saturation and error constraints," IET INTELL TRANSP SY, vol. 14, no. 5, pp 356-363, 2019.

[7]. Jin Jiang and Xiang Yu, "Fault-tolerant control systems: A comparative study between active and passive approaches," ANNU REV CONTROL, vol. 36, no. 1, pp 60-72, 2012.

[8]. Qiang Shen, Chengfei Yue and Cher Hiang Goh, "Active Fault-Tolerant Control System Design for Spacecraft Attitude Maneuvers with Actuator Saturation and Faults," IEEE T IND ELECTRON, vol. 66, no. 5, pp 3763-3772, 2018.

[9]. Bing Xiao, Mingyi Huo and Xuebo Yang, "Fault Tolerant Attitude Stabilization for Satellites Without Rate Sensor," IEEE T IND ELECTRON, vol. 62, no. 11, pp 7191-7202, 2015.

[10]. Teng Cao, Zhifeng Gao and Moshu Qian, "Passive Fault Tolerant Control Approach for Hypersonic Vehicle with Actuator Loss of Effectiveness Faults," 2016 28th Chinese Control and Decision Conference (CCDC), 2016

[11]. Mou Chen, Peng Shi and Cheng-Chew Lim, "Adaptive Neural Fault-Tolerant Control of a 3-DOF Model Helicopter System," IEEE T SYST MAN CY-S, vol. 46, no. 2, pp 260-270, 2015.

[12]. J. W. Zhu, G. H. Yang, H. Wang, and F. L. Wang, "Fault estimation for a class of nonlinear systems based on intermediate estimator," IEEE T AUTOMAT CONTR, vol. 61, no. 9, pp. 2518–2524, 2016.

[13]. Chunyue Li, Jiajia Jiang, Fajie Duan, "Modeling and Experimental Testing of an Unmanned Surface Vehicle with Rudderless Double Thrusters," SENSORS-BASEL, vol. 19, no. 9, 2019.